Supporting Information

Highly Ordered $ZnO/ZnFe_2O_4$ Inverse Opals with Binder-free Heterojunction Interfaces for High-performance Photoelectrochemical Water Splitting

Tingting Yang,[a+] Jiawei Xue,[b+] Hao Tan,[b] Anjian Xie,[a] Shikuo Li,[a*] Wensheng Yan,[b] Yuhua Shen[a*]

[a] Lab of Clean Energy & Environmental Catalysis, School of Chemistry and Chemical Engineering, Anhui University, Hefei 230601, China

[b] National Synchrotron Radiation Laboratory, University of Science and Technology of China, Hefei, 230029, P.R. China

[+] These authors contributed equally to this work.

Received (in XXX, XXX) Xth XXXXXXXXX 20XX, Accepted Xth XXXXXXXXX 20XX

DOI: 10.1039/b000000x

Experimental Section

Synthesis of monodisperse polystyrene spheres

Monodisperse polystyrene (PS) latex spheres were synthesized by emulsifier-free emulsion copolymerization technique according to the literature[1] using styrene as polymerized monomer, and potassium persulfate (KPS) as initiator. Styrene (210 mL) was washed in a separatory funnel four times with 200 mL of 0.1 M NaOH, then four times with 200 mL of water. The synthetic process was modified in our laboratory. In a typical synthesis of monodisperse PS latex spheres with 300 nm diameter was as follows: Polymerization was conducted in a 250 mL reaction flask by magnetic stirring (350 rpm) under a nitrogen atmosphere. Firstly, 100 mL deionized water was added to a three-neck flask. Nitrogen was bubbled in the flask to blow away air. After 30 min, 6.2 mL prewashed styrene was added to the flask. Then, the reaction flask was heated to 75 °C, 0.1 g prepurified KPS was added. After the reaction of 24 h, the flask was removed from the oil bath. The subsequently formed white latex was filtrated through glass filter to remove aggregates, and centrifuged, washed with deionized water for several times, finally the precipitate dispersed into water for use.

Hydrogen and oxygen evolution measurements

The photogenerated hydrogen and oxygen by PEC water splitting was performed in an air-tight reactor connected to a closed gas circulation system (Beijing China Education Au-light Co., Ltd). Prior to measurements, the cell compartments were carefully sealed with rubber septa and glycerin to prevent any gas leakage and then Ar-purged for 1 h. During measurements, the as-prepared of $ZnO/ZnFe_2O_4$ sample used as photoanodes were biased at 1.23 V *vs* RHE in a stirred aqueous solution of 0.1 M Na_2SO_4 under AM 1.5G simulated sunlight. The amounts of hydrogen or oxygen

were determined by gas chromatography (GC-3240) equipped with a thermal conductivity detector (TCD), and ultrahigh purity argon (Linde, 99.9995%) as carrier gas. The Faradaic efficiency of the as-prepared of $ZnO/ZnFe_2O_4$ sample can be calculated from hydrogen and oxygen evolution measurements by the following formula:

$$Faradaic\ efficiency(\%) = znF / Q \times 100\%$$

where z is the number of electron gain-loss (for example, $2H^+$ back to H_2, z is 2), n is amount of substance of H_2 and O_2 (mol), F is the Faraday constant (96500 C/mol), and Q is the total charge.

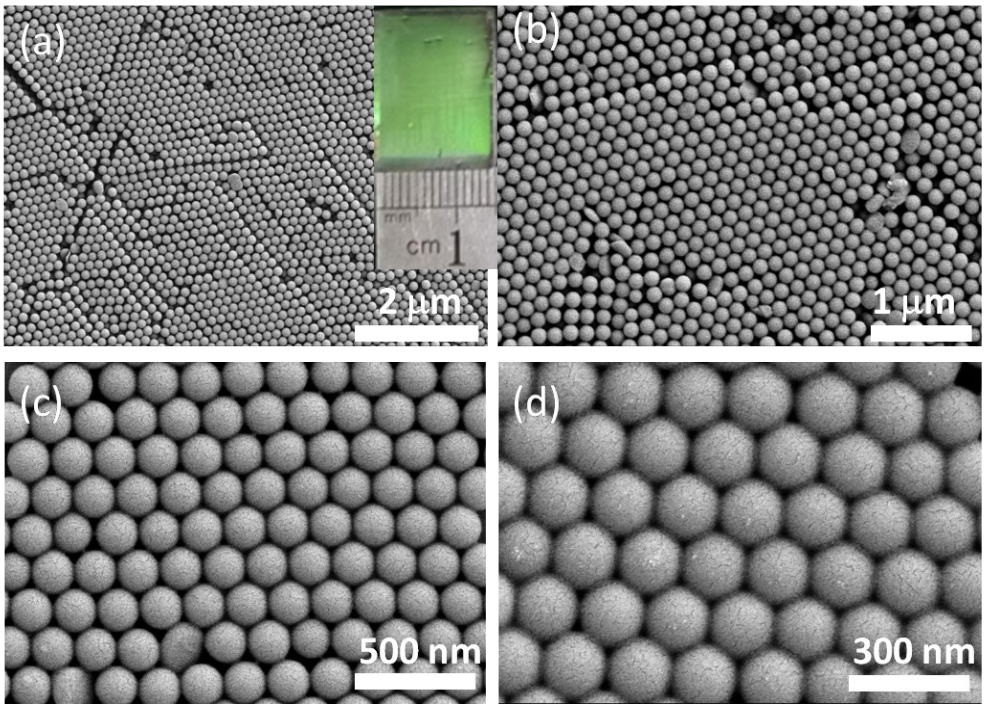

Figure S1. (a-d) Different magnification SEM images of PS template, the inset is the photo of the PS film.

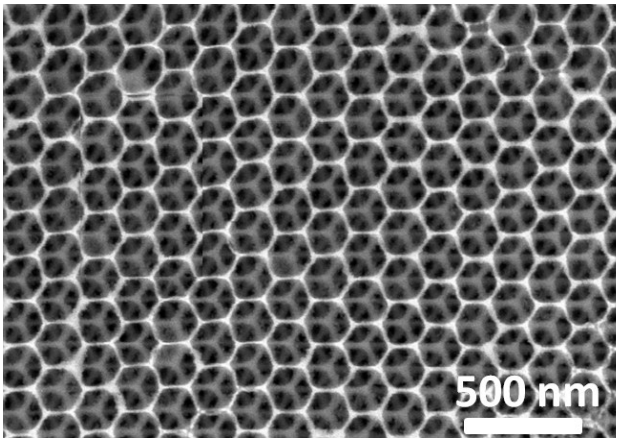

Figure S2. SEM image of ZnO inverse opal prepared by removing the PS template.

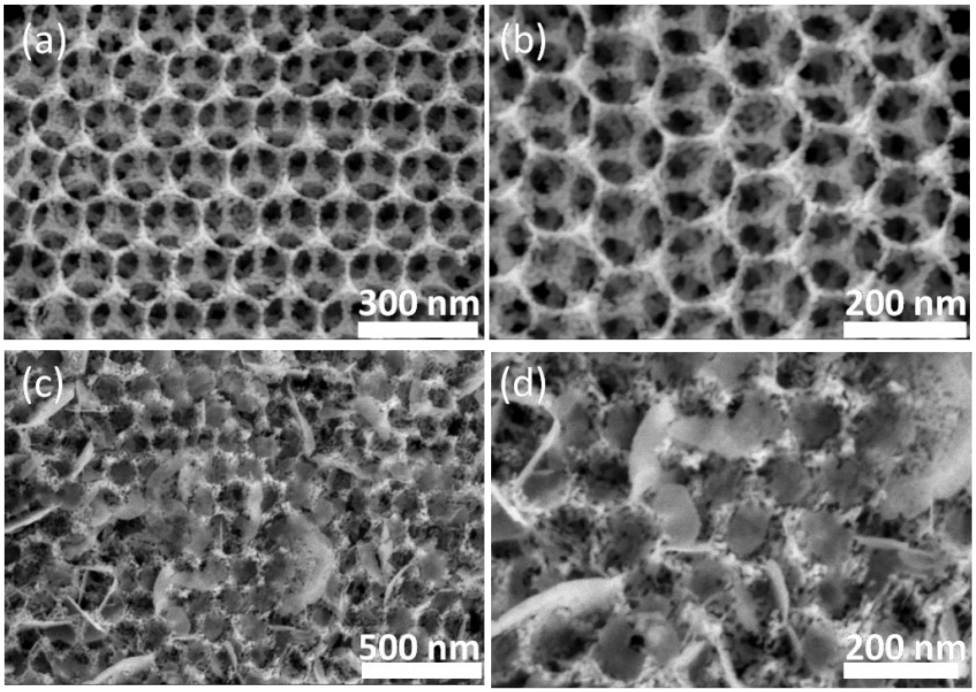

Figure S3. SEM images of ZnO/$ZnFe_2O_4$ inverse opal samples prepared with different dip coatings (a, b) 30 cycles, and (c, d) 120 cycles.

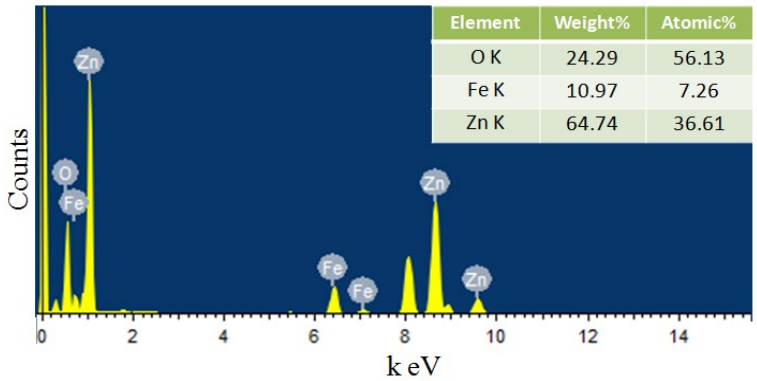

Figure S4. EDX spectra of the typical ZnO/$ZnFe_2O_4$ inverse opal sample prepared with 60 dip coating cycles.

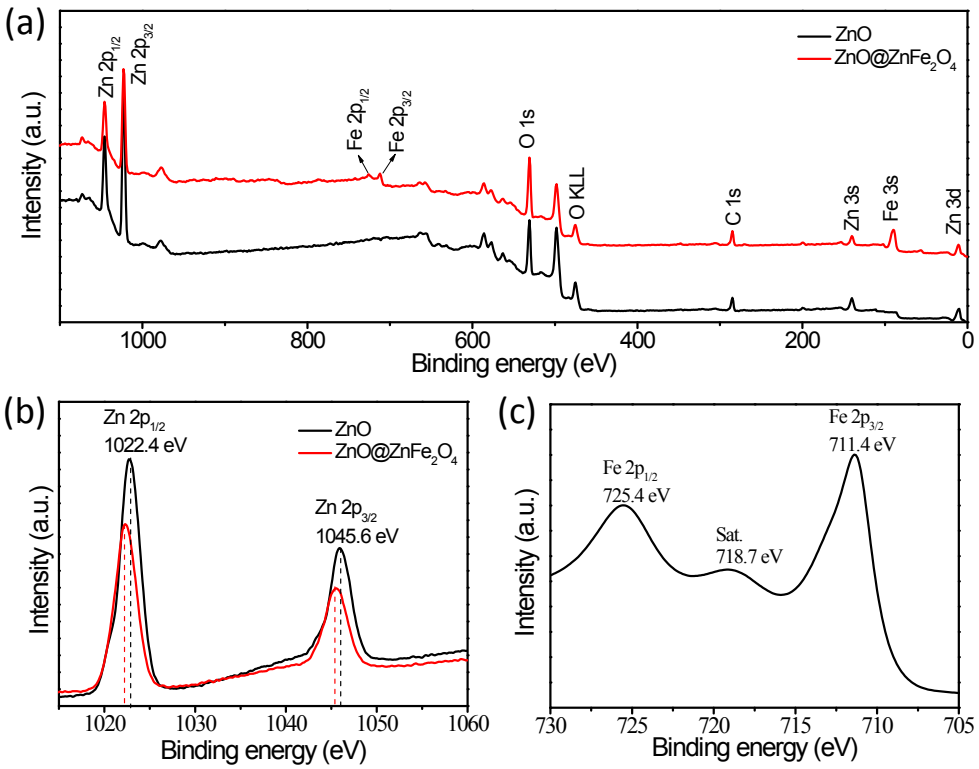

5 **Figure S5**. XPS survey spectra (a), Zn 2p (b), and (c) Fe 2p of the pristine ZnO and the typical ZnO/$ZnFe_2O_4$ inverse opal prepared with 60 dip coating cycles.

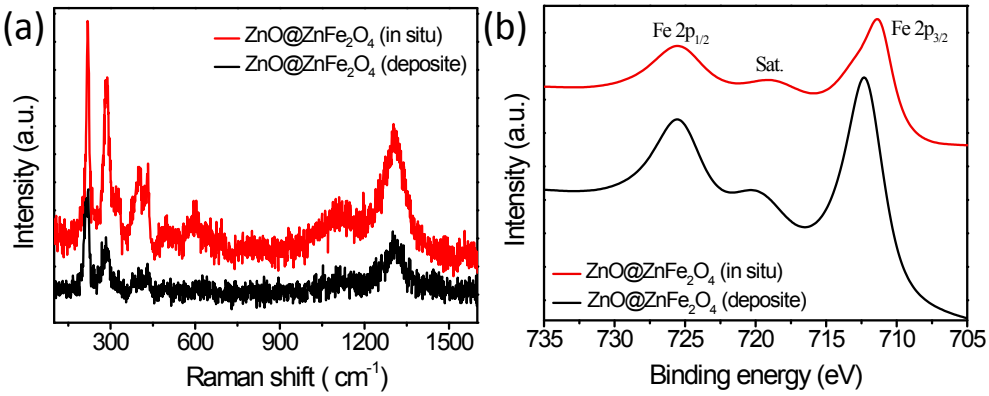

Figure S6. Raman spectra (a), and Fe 2p XPS spectra (b) of the different ZnO/$ZnFe_2O_4$ samples.

The Raman spectra of different ZnO/$ZnFe_2O_4$ samples were characterized as shown in Figure S6a. The peak at 437 cm^{-1} was assigned to the normal E_{2H} mode of ZnO. The peak at 379 cm^{-1} arise from the A_{1T} modes, respectively, whilst the mode at 593 cm^{-1} correspond to E_{1L}, respectively.[2] The other peaks at 220, 288, 402, 488, 602 cm^{-1} can match the characteristic vibrations of Fe_2O_3.[3] The intensity of the peaks in the mixed samples were weaker than that of the *in situ* transformed samples, suggesting $ZnFe_2O_4$ coating on the surface of ZnO in the transformed samples. Figure S6b exhibited the Fe 2p XPS spectra of different ZnO/$ZnFe_2O_4$ samples. It can be seen that the Fe 2p1/2 peak obviously shifted to a lower energy level compared to the $ZnFe_2O_4$ deposited on ZnO composite sample, confirming the presence of strong interfacial interactions in the *in situ* transformed ZnO/$ZnFe_2O_4$ sample. It is in agreement with the results of Figure 1d. The strong interfacial interactions are in favor of electron fluently transferring through their interface.

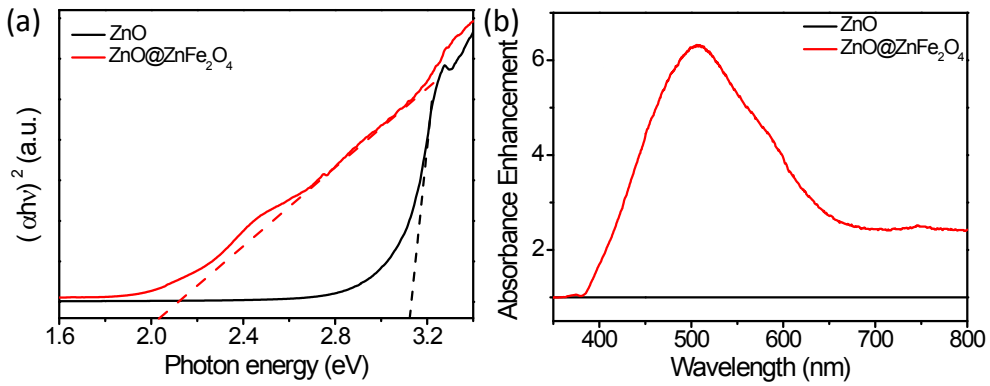

Figure S7. (a) Plots of $(\alpha h\nu)^2$ versus photo energy (eV), and (b) Absorbance enhancement factor curves of pristine ZnO and ZnO/$ZnFe_2O_4$ inverse opal prepared with 60 dip coating cycles.

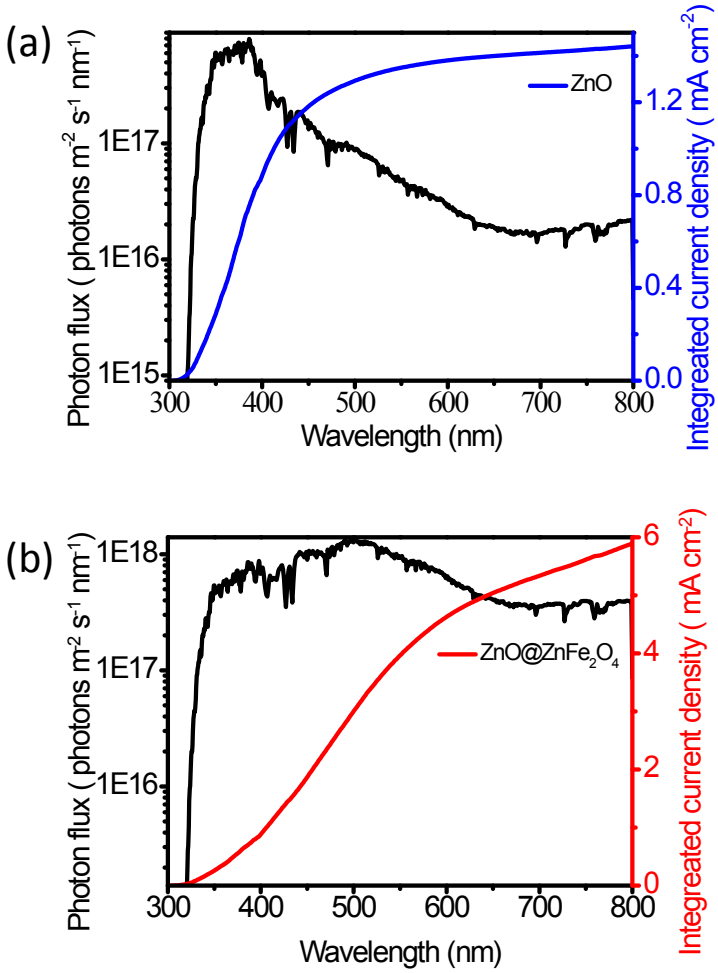

Figure S8. Integrated current densities for the pristine ZnO (a) and typical $ZnO/ZnFe_2O_4$ prepared with 60 dip coating cycles (b) inverse opal samples as a function of wavelength, by integrating their UV−vis absorption spectra with a standard AM 1.5G solar spectrum (ASTM G-173-03).

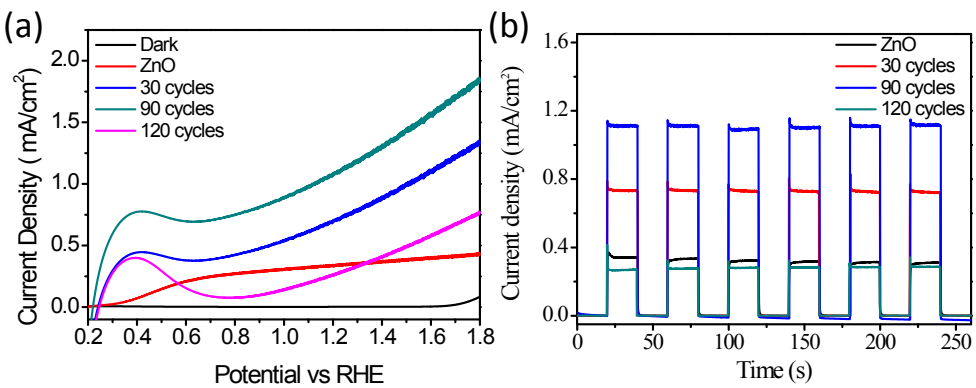

Figure S9. J-V curves under AM 1.5 G simulated sunlight at a scan rate of 10 mV s^{-1} in 0.1 M Na_2SO_4 solution (a), and Amperometric *I*−*t* curves under chopped light irradiation with on/off interval of 20 s at 1.23 V *vs* RHE (b) of $ZnO/ZnFe_2O_4$ inverse opal samples prepared with different dip coating cycles.

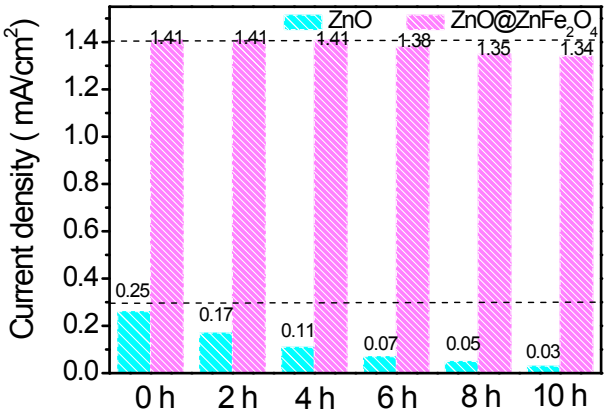

Figure S10. The photocurrent retention ratio of the pristine ZnO and the typical ZnO/$ZnFe_2O_4$ inverse opal prepared with 60 dip coating cycles under continuous AM 1.5G illumination at 1.23 V *vs* RHE for 10 h.

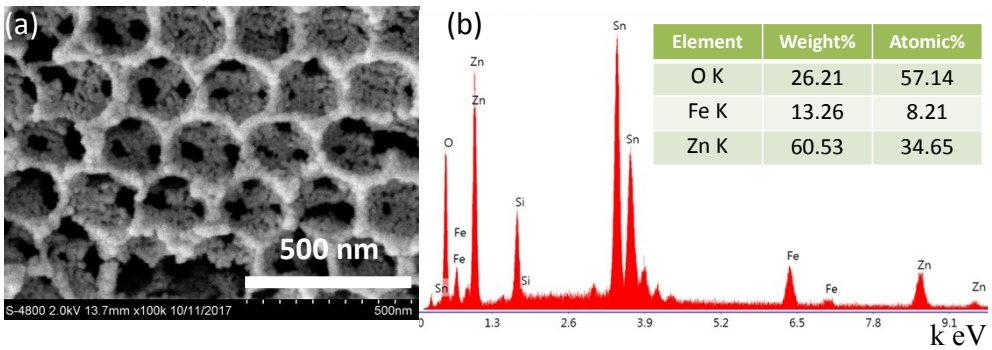

5 Figure S11. (a) SEM image, and (b) EDX spectrum of the typical ZnO/$ZnFe_2O_4$ inverse opal prepared with 60 dip coating cycles under continuous AM 1.5G illumination at 1.23 V *vs* RHE for 10 h.

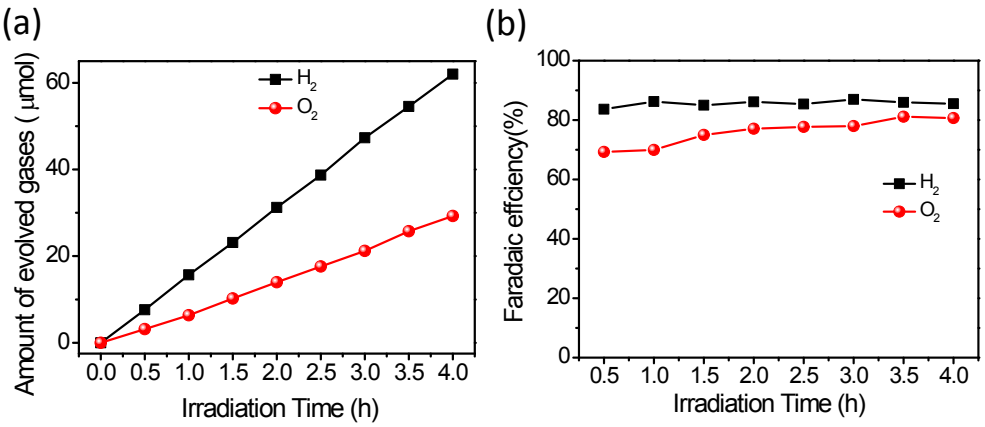

Figure S12. (a) H_2 and O_2 evolution curves measured at 1.23 V vs. RHE under AM 1.5G, and (b) Faradaic efficiency curves of the generated H_2 and O_2 from the as-prepared typical ZnO/$ZnFe_2O_4$ inverse opal electrode.

10 H_2 and O_2 evolution reactions of the as-prepared typical ZnO/$ZnFe_2O_4$ inverse opal electrode were measured as shown in **Figure S12**. The as-prepared typical ZnO/$ZnFe_2O_4$ inverse opal generated 62.2 μmol cm^{-2} and 29.5 μmol

cm^{-2} H_2 and O_2, respectively, at 1.23 V vs. RHE under AM 1.5G for 4 h. The ratio of the H_2 and O_2 was near the stoichiometric value of 2.0. The obtained Faradaic efficiencies of 85.3% and 77.6% as shown in **Figure S12b** determined by the measurement of the evolved H_2 and O_2 gas, respectively, suggesting that the photocurrent is indeed aroused by the oxygen evolution reaction and hydrogen evolution reaction.

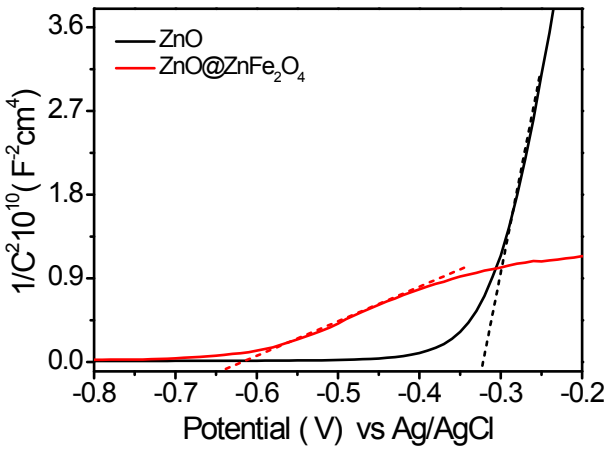

Figure S13. Mott–Schottky plots measured in the DC potential range from -0.4 V to 0.4 V vs. RHE at a frequency of 10 kHz of the pristine ZnO and the typical ZnO/ZnFe2O4 inverse opal prepared with 60 dip coating cycles in the dark.

Based on the above HRTEM results of the $ZnO@ZnFe_2O_4$ heterojunction interfaces, ZnO (100) surface and $ZnFe_2O_4$ (111) surface were modelled for computational simulations. For a ZnO unit cell, the space group is P 63 M C, with lattice parameter $\alpha = \beta = 90°$, $\gamma = 120°$ and a = b = 3.25Å, c = 5.21 Å. For $ZnFe_2O_4$ unit cell, the space group is F D -3 M, with lattice parameter $\alpha = \beta = \gamma = 90°$ and a = b = c = 8.35 Å. To minimize the lattice mismatch, a $(\sqrt{3} \times 2)$ $ZnFe_2O_4$ (111) slab with a thickness of six atom layers which contains 8 Zn atoms, 16 Fe atoms and 32 O atoms were built to match a (4 × 4) ZnO (100) slab with a thickness of four layers which contains 32 Zn atoms and 32 O atoms. All of the calculations were been performed using the computational software Materials Studio. A Hubbard-like, localized term was added to the local density approximation (LDA), which was called (LDA+U), and was used to describe the exchange-correlation effects and electron ion interactions, respectively. The value of U was set to 8.0 and 6.8 eV for Zn and Fe, respectively. The vacuum slab perpendicular to the surface models was 15 Å, which was enough to separate the interaction between periodic images. We used a 4 × 5 × 1 Monkhorst-Pack k-point mesh for geometry optimization and a 4 × 4 × 1 mesh to calculate its density of states. The cutoff energy for planewave was been chosen to be 340 eV. In the geometry optimization process, the energy change, maximum force, maximum stress and maximum displacement tolerance values were set to 1×10^{-5} eV per atom, 0.03 eV $Å^{-1}$, 0.05 GPa, and 0.001 Å, respectively.

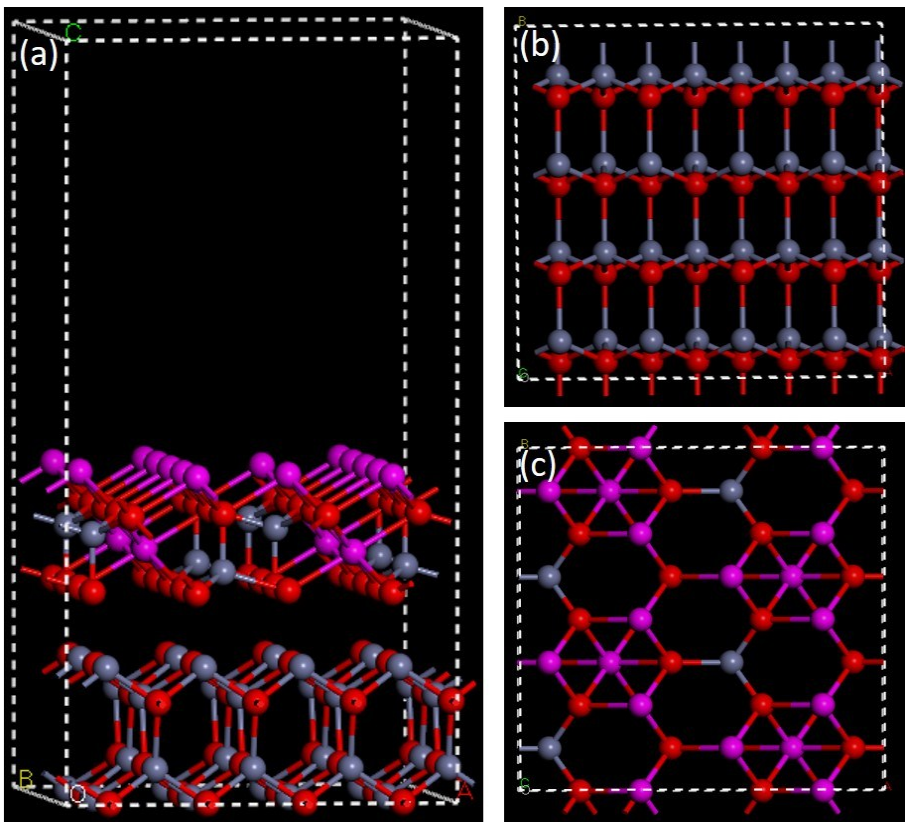

Figure S14. (a) Side-view geometry of the $ZnO@ZnFe_2O_4$ interface model, (b) Top-view geometry of the ZnO (100) surface model, and (c) Top-view geometry of the $ZnFe_2O_4$ (111) surface model. The gray, pink, and red spheres represent Zn, Fe, and O atoms, respectively.

Table S1. Comparison of the $ZnO/ZnFe_2O_4$ inverse opal electrode in this work with previously reported $ZnFe_2O_4$-based photonaodes toward PEC water splitting.

Samples	Photocurrent @1.23V(*vs.* RHE) /mA cm^{-2}	Maximum photoconversion Efficiency %	Stability (*vs.* RHE)	Electrolyte	Reference
$TiO_2/ZnFe_2O_4$ nanotrees	0.85	0.31	N.A.	1 M KOH	4
$ZnFe_2O_4$ films	0.1	0.021	N.A.	0.1 M NaOH	5
$SrTiO_3/ZnFe_2O_4$ films	0.188	N.A.	3 h at 1.23 V	1 M NaOH	6
$Ag/ZnO/ZnFe_2O_4$ porous films	0.013	N.A.	N.A.	0.5 M Na_2SO_4	7
ZnO/TiO_2/FeOOH nanowires	1.2	0.36	2h at 1.1 V	0.5 M Na_2SO_4	8
$Au/ZnFe_2O_4$/ZnO nanorods	0.85	0.35	N.A.	0.1 M Na_2SO_4	9
$ZnFe_2O_4$ nanorods	0.35	N.A.	3h at 1.23 V	1 M NaOH	10
Al-treated $Fe_2O_3/ZnFe_2O_4$	0.38	N.A.	N.A.	1 M NaOH	11
$ZnFe_2O_4$ nanorods	0.25	N.A.	3h at 1.23 V	1 M NaOH	12
$ZnO@ZnFe_2O_4$ inverse opal networks	1.4	0.81	loss 4.9% after 10h at 1.23 V	0.1 M Na_2SO_4	This work

These electrodes were tested under AM 1.5 G simulated sunlight (100 mW cm^{-2}).

References

1. Holland B T, Blanford C F, Do T, et al, *Chem. Mater.* 1999, **11**, 795-805.
2. Y. Li, G. Dai, C. Zhou, Q. Zhang, Q. Wan, L. Fu, J. Zhang, R. Liu, C. Cao, A. Pan, Y. Zhang and B. Zou, *Nano Research*, 2010, **3**, 326-338.
3. Y. Guo, Y. Fu, Y. Liu and S. Shen, *RSC Advances*, 2014, **4**, 36967-36972.
4. S. Shen, S. A. Lindley, X. Chen and J. Z. Zhang, *Energy Environ. Sci.*, 2016, **9**, 2744-2775.
5. F. Ning, M. Shao, S. Xu, Y. Fu, R. Zhang, M. Wei, D. G. Evans and X. Duan, *Energy Environ. Sci.*, 2016, **9**, 2633-2643.
6. S. Cao, X. Yan, Z. Kang, Q. Liang, X. Liao and Y. Zhang, *Nano Energy*, 2016, **24**, 25-31.
7. M. Wu, W. J. Chen, Y. H. Shen, F. Z. Huang, C. H. Li and S. K. Li, *ACS Appl. Mater. Inter.*, 2014, **6**, 15052-15060.
8. S. Meng, D. Li, X. Fu and X. Fu, *J. Mater. Chem. A*, 2015, **3**, 23501-23511.
9. M. Zhou, H. B. Wu, J. Bao, L. Liang, X. W. Lou and Y. Xie, *Angew. Chem.*, 2013, **52**, 8579-8583.
10. M. Ma, J. K. Kim, K. Zhang, X. Shi, S. J. Kim, J. H. Moon and J. H. Park, *Chem. Mater.*, 2014, **26**, 5592-5597.
11. M. Zalfani, B. van der Schueren, Z.-Y. Hu, J. C. Rooke, R. Bourguiga, M. Wu, Y. Li, G. Van Tendeloo and B.-L. Su, *J. Mater. Chem. A*, 2015, **3**, 21244-21256.
12. J. H. Kim, Y. J. Jang, J. H. Kim, J. W. Jang, S. H. Choi and J. S. Lee, *Nanoscale*, 2015, **7**, 19144-19151.